

Article

A Coupled Simulated Annealing and Particle Swarm Optimization Reliability-Based Design Optimization Strategy under Hybrid Uncertainties

Shiyuan Yang^{1,2}, Hongtao Wang^{1,2}, Yihe Xu³, Yongqiang Guo⁴, Lidong Pan⁴, Jiaming Zhang⁴, Xinkai Guo², Debiao Meng^{1,2,*}  and Jiapeng Wang¹

¹ School of Mechanical and Electrical Engineering, University of Electronic Science and Technology of China, Chengdu 611731, China

² Institute of Electronic and Information Engineering of UESTC in Guangdong, Dongguan 523808, China

³ Glasgow College, University of Electronic Science and Technology of China, Chengdu 611731, China

⁴ Beijing Research Institute of Mechanical & Electrical Technology Ltd., Beijing 100083, China

* Correspondence: dbmeng@uestc.edu.cn

Abstract: As engineering systems become increasingly complex, reliability-based design optimization (RBDO) has been extensively studied in recent years and has made great progress. In order to achieve better optimization results, the mathematical model used needs to consider a large number of uncertain factors. Especially when considering mixed uncertainty factors, the contradiction between the large computational cost and the efficiency of the optimization algorithm becomes increasingly fierce. How to quickly find the optimal most probable point (MPP) will be an important research direction of RBDO. To solve this problem, this paper constructs a new RBDO method framework by combining an improved particle swarm algorithm (PSO) with excellent global optimization capabilities and a decoupling strategy using a simulated annealing algorithm (SA). This study improves the efficiency of the RBDO solution by quickly solving MPP points and decoupling optimization strategies. At the same time, the accuracy of RBDO results is ensured by enhancing global optimization capabilities. Finally, this article illustrates the superiority and feasibility of this method through three calculation examples.

Keywords: reliability-based design and optimization; particle swarm optimization algorithm; simulated annealing algorithm; most probable point

MSC: 60C05; 65Y04; 65Y20; 62D05



Citation: Yang, S.; Wang, H.; Xu, Y.; Guo, Y.; Pan, L.; Zhang, J.; Guo, X.; Meng, D.; Wang, J. A Coupled Simulated Annealing and Particle Swarm Optimization Reliability-Based Design Optimization Strategy under Hybrid Uncertainties. *Mathematics* **2023**, *11*, 4790. <https://doi.org/10.3390/math11234790>

Academic Editors: Janez Žerovnik and Carlos Conceicao Antonio

Received: 20 October 2023

Revised: 18 November 2023

Accepted: 25 November 2023

Published: 27 November 2023



Copyright: © 2023 by the authors. Licensee MDPI, Basel, Switzerland. This article is an open access article distributed under the terms and conditions of the Creative Commons Attribution (CC BY) license (<https://creativecommons.org/licenses/by/4.0/>).

1. Introduction

The construction of engineering systems will inevitably be affected by complex uncertain factors [1–3]. Especially with the increasing complexity of engineering systems, various uncertainties will be mixed and difficult to distinguish [4]. If these factors cannot be analyzed accurately, the reliability and security of the engineering system cannot be guaranteed [5–8]. At present, the Reliability-Based Design Optimization (RBDO) method has been widely used to improve the reliability and safety of complex mechanical systems [9]. However, with the growth of social demand, new technology should be introduced constantly to improve the development level of reliability optimization design and meet the needs of economic development for engineering [10].

RBDO takes into account the inevitable random factors in engineering systems [11–14]. It ensures that the reliability of the object system is within an acceptable range by optimizing the objective function [15]. It is an extension of deterministic optimization methods and is used to solve complex uncertain engineering system optimization problems [16,17]. In recent years, RBDO has been discussed and studied by a large number of scholars. Many

algorithms and models have been developed to solve the RBDO problem. Liao et al. [18] adopted an improved double-loop calculation method to improve the computational efficiency of the RBDO model. In this method, RBDO is divided into two layers and is calculated step by step through reliability analysis (RA) and deterministic optimization (DO). The optimization strategy of this double-loop method usually has a low optimization rate. Wang et al. [19] proposed an improved Modified Conjugate Gradient Approach (MCGA) to improve the RBDO efficiency of nonlinear function functions. This method uses the improved conjugate gradient method (CGA) to search the most probable point (MPP) point direction, which improves the efficiency of RBDO. At the same time, unlike gradient algorithms, metaheuristic algorithms are widely used in RBDO methods. Safaeian et al. used the particle swarm algorithm (PSO) [20] combined with a weighted simulation-based design method for design optimization, which improved the accuracy of the RBDO method and the ability to solve general RBDO problems. However, this method uses a double-loop method to solve the problem, which is less efficient. Zhong et al. used a Harris Hawks Optimization algorithm [21], which has a higher efficiency in solving the global optimal solution. Since the derivative of the limit state function is not required, this method has a higher calculation speed, but its accuracy still has room for improvement. Jafar et al. [22] improved the previous Harris Hawks Optimization algorithm and transformed the problem of solving unit vectors with a highly nonlinear performance function into a constrained optimization problem, which greatly improved the solution efficiency of this method.

The above algorithm does not consider mixed uncertainties. However, studies have long found that mixed uncertainty also has a great impact on the analysis of engineering systems [23]. In recent years, engineering problems considering mixed uncertainties have been extensively studied. Such problems containing multiple uncertainties pose challenges to the optimization efficiency and difficulty of RBDO. Zhang et al. [24] proposed a hybrid uncertainty analysis method based on probability and evidence theory, which improved the efficiency of RBDO analysis. Wang et al. [25] proposed an RBDO solution strategy that relies on conditioning processing and convexity theorem. This method uses an improved genetic algorithm and has a relatively good application effect on optimization tasks that consider time-varying and time-invariant mixed variables. However, this method is only suitable for time-related RBDO problems. Thu et al. [26] used the PSO algorithm combined with the Gaussian process to propose a new reliability design optimization method. This method utilizes the excellent global optimization capabilities of the PSO method, but its optimization capabilities for engineering problems that consider uncertainty are yet to be discussed. As shown in Figure 1, the methods used in past studies are demonstrated. Due to space limitations, only typical algorithm strategies are selected to demonstrate the development process.

After the literature research, it was found that the PSO method can better solve the problem of local convergence in the analysis process than other heuristic algorithms. Compared with the double-loop method with huge computational cost and the single-loop method optimization algorithm with difficulty in ensuring the optimization accuracy of high-dimensional nonlinear problems, the decoupled optimization strategy combined with the computationally efficient simulated annealing (SA) algorithm has a higher solution speed. This study combines these two optimization algorithms and proposes a new RBDO method. It is used to solve the RBDO problem of high-dimensional nonlinear engineering structures considering mixed uncertainties. This method is dedicated to solving the purpose of improving the accuracy and computational efficiency of optimization results during the optimization process.

The rest of the parts of this paper include: Section 2 summarizes the PSO algorithm and SA algorithm; Section 3 illustrates the idea of combining the two algorithms. Section 4 verifies and compares with other methods through examples; Section 5 provides a summary and future work.

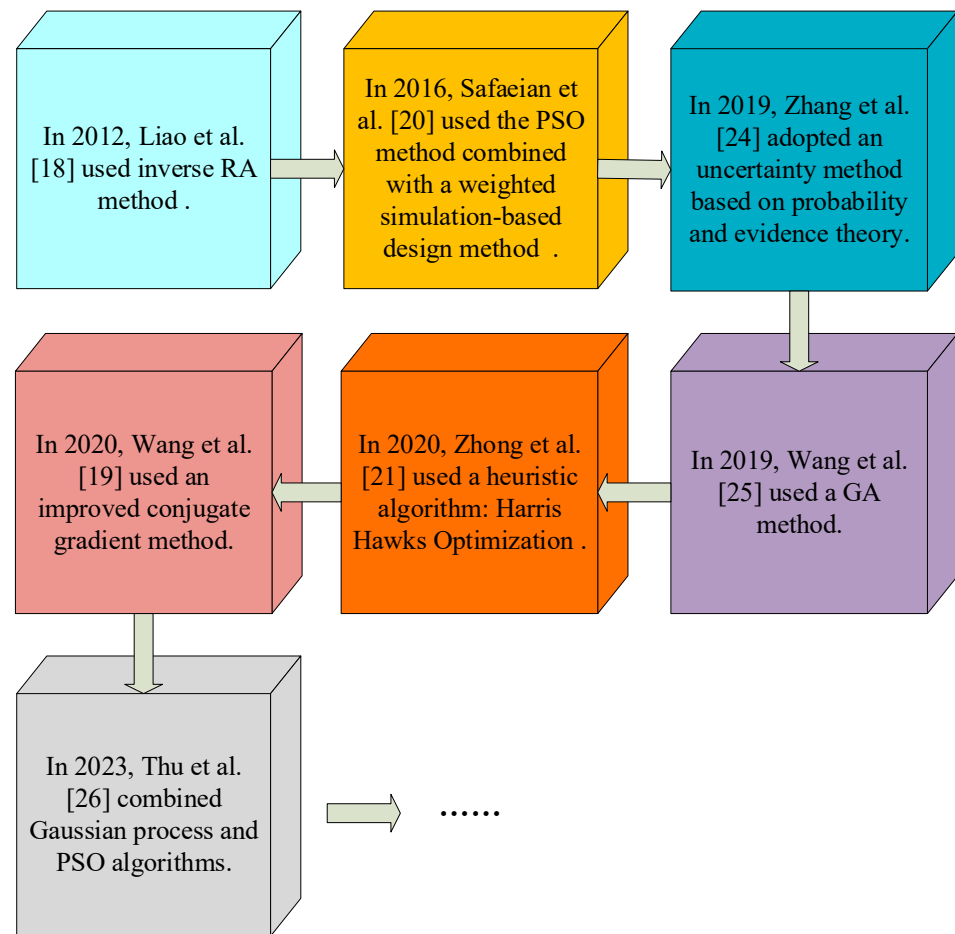


Figure 1. Development history of algorithm strategies in engineering structure analysis and optimization.

2. Two Algorithms for Optimizing the Problem

2.1. Particle Swarm Optimization

2.1.1. Definition of Particle Swarm Optimization

PSO also known as the foraging algorithm, is a widely used meta-heuristic algorithm, which is derived from the study of bird predation behavior [27,28]. The algorithm is originally a simplified model based on swarm intelligence inspired by the regularity of bird swarm activity. Based on the observation of the activity behavior of animal clusters, the PSO algorithm makes use of the information sharing of each individual in the group, so that the movement of the whole group can evolve from disorder to order in the problem-solving space [29,30]. Finally, it can obtain the optimal solution successfully.

In PSO, the optimal solution is generated by reducing the distance between each search individual and the target point [31]. Under this goal, the position of the particle varies depending on two factors: the velocity of the particle and the current position of the particle. During the search for the optimal solution, the velocity of the particle and the current position of the particle are constantly changing. The value of velocity is determined by the particle with the optimal current position and the particle with the optimal global position. Its mathematical expression is

$$\begin{cases} V_{k+1} = wV_k + c_1r_1(p_{best} - X_k) + c_2r_2(g_{best} - X_k) \\ X_{k+1} = X_k + V_{k+1} \end{cases} \quad (1)$$

where V_k represents the particle velocity of k iterations; X_k represents the particle position of k iterations; w represents inertia weight; p_{best} represents the optimal value of the particle at its current position; g_{best} represents the global optimal value; c_1, c_2 , respectively represent

individual learning coefficient and global learning coefficient; r is a random value between 0 and 1, called the learning rate.

In the process of iteration, speed boundary detection should be carried out after each speed update, that is, whether the maximum speed limit is exceeded. Generally, adopting $v(v > v_{\max}) = v_{\max}$, so as the location. The common termination conditions are reaching the set number of iterations and keeping the fitness for n times without changing [32].

2.1.2. Optimization of PSO Algorithm

Equation (1), w describes the “inertia” of particles. In the early stage of iteration, the value of w should be larger to ensure the independent flight of each particle and to search the space as fully as possible. In the later stage of iteration, the value of w should be smaller and more “learned” from other particles. Similarly, c_1 and c_2 are the maximum flight steps toward individual and global extremes, respectively. c_1 should be larger in the early stage, while c_2 should be larger in the late stage, to balance the local search ability and global search ability of particles. In the PSO algorithm, the parameters w , c , and r jointly affect the search direction of particles. So even if other particles find a better solution, the inertia of the current particles is too large to fly to a better position quickly.

Against the deficiency of standard particle swarm algorithm, through the introduction of new mechanism and parameter optimization of adaptive changes of PSO algorithm [33]. Firstly, the parameter optimization of the PSO algorithm. As mentioned above, the inertia weight w should be larger in the early stage of search and smaller in the late stage, so that particles can search the entire design space as much as possible in the early stage and more carefully in the late stage. For this optimization strategy, the inertia weight w is adjusted as follows [30]:

$$w_k = w_{\min} + \frac{ger - k}{ger}(w_{\max} - w_{\min}), \tag{2}$$

where w_k represents the inertia weight at each iteration; w_{\min} and w_{\max} , respectively, denote the lower and upper bounds of the inertia weight; k represents the number of current iterations; ger represents the total number of iterations; as can be seen from the expression of w_k , the value of inertia weight w_k decreases monotonically, realizing the function of decreasing gradually with the process of search. Similarly, the same optimization strategy is adopted for the learning coefficient c . The expression of the optimized c_1 and c_2 is shown as follows:

$$\begin{cases} c_{k1} = c_{\min} + \frac{ger - k}{ger}(c_{\max} - c_{\min}) \\ c_{k2} = c_{\max} - \frac{ger - k}{ger}(c_{\max} - c_{\min}) \end{cases}, \tag{3}$$

where c_{k1} represents the individual learning coefficient in each iteration; c_{k2} represents the global learning coefficient of each iteration. In addition, the learning rate r is no longer a random value between 0 and 1, but a random variable subject to the standard normal distribution, namely $r \sim (0, 1)$.

Secondly, to make the search process avoid falling into local optima and focus more on global optima, an additional method of updating particle position X and velocity V are used for reference here. The method is as follows:

$$\begin{cases} X_{k+1} = X_k + V_{k+1}^E \\ V_{k+1}^E = r_3(g_{best} - X_k) + Normrand(0, 1) \times \gamma_k \\ \gamma_k = \sqrt{1 - k/ger} \end{cases}, \tag{4}$$

where the new position is calculated by the global optimal value and the random number obeying the normal distribution. r_3 is a random number between 0 and 1; $Normrand(0, 1)$ is a randomly generated vector conforming to the standard normal distribution; γ_k is an adaptively variable step that changes the size of the random value.

As can be seen from the expression of V_{k+1}^E , since a random value is introduced, the probability of falling into a local optimal when updating the position can be reduced.

However, the efficiency of the search will decrease accordingly in the meantime. In order to balance the two results, a new decision mechanism is introduced here:

$$X_{k+1} = \begin{cases} X_k + V_{k+1}^E, r \leq P_k \\ X_k + V_{k+1}, r > P_k \end{cases}, \tag{5}$$

where r is a random number between 0 and 1; P_k represents the probability of the particle choosing two position updating modes. The expression is

$$P_k = 0.2 + 0.8\sqrt{k/ger}. \tag{6}$$

As can be seen from the expression of P_k , with the progress of iteration, the value of P_k keeps increasing, which makes the probability of using V_{k+1}^E to update the speed of V correspondingly increase.

This mechanism for updating particle positions ensures that the particle is more focused on the global optimal value later in the search process. This improves the efficiency to some extent and reduces the probability of falling into local optimal.

2.2. Simulated Annealing Algorithm

2.2.1. Definition of Simulated Annealing Algorithm

The annealing process of a metal involves heating the metal to a sufficiently high temperature and then letting it slowly cool down to give the metal some properties it did not have before [34–36]. When the temperature increases, the particles inside the solid become disordered as the temperature increases. An increase in internal energy then occurs and the particles become unstable. The particles gradually become orderly when slowly cooled. As the energy decreases, the particles become stable [37]. The simulated annealing algorithm starts from a higher initial temperature. With the continuous decline of temperature parameters, the algorithm combines the probability jump characteristics to randomly find the global optimal solution of the objective function in the solution space.

2.2.2. Simulated Annealing Algorithm

The SA mechanism can avoid falling into local optimum to some extent. Different from many intelligent optimization algorithms, the SA algorithm will jump to the solution with a certain probability. Even if it finds a worse solution than the current solution in the process of local search, it can avoid falling into the local optimal [38]. This way of updating solutions requires an important judgment criterion called the Metropolis criterion:

$$P = \begin{cases} 1, E_{t+1} < E_t \\ e^{-\frac{(E_{t+1}-E_t)}{kT}}, E_{t+1} \geq E_t \end{cases} \tag{7}$$

where P is the probability of accepting the new solution; E_t is the system energy corresponding to the current solution X_t (objective function); k is the temperature drop coefficient, which is a value between 0 and 1. T indicates the initial temperature. Based on this criterion, it can be concluded that (here is to find the minimum value):

- (1) When the objective function corresponding to the new solution is less than the objective function value of the current solution, it will accept the new solution. That is, the probability of accepting the new solution is 1;
- (2) When the corresponding objective function of the new solution is greater than the objective function value of the current solution, the new solution will be accepted with a certain probability. When other variables are certain, the more the value of the objective function corresponding to the new solution exceeds the value of the objective function of the current solution, the smaller the probability of accepting the new solution.

The steps of the SA algorithm are as follows:

- Step 1: Set the initial temperature T ; The initial solution X_0 is generated randomly and the objective function $E(X_0)$ is calculated;
- Step 2: Make $T = kT, k \in (0, 1)$;
- Step 3: Make random perturbation to the current solution X_t , generate a new solution X_{t+1} in its field, and calculate its corresponding function value $E(X_{t+1})$. Meanwhile, judge whether to accept the new solution according to the Metropolis criterion above;
- Step 4: At temperature T , iterate the disturbance and acceptance process for L times;
- Step 5: Determine whether the terminal temperature is reached. If so, terminate; otherwise, return to step 2.

3. The Combination of Intelligent Algorithms

3.1. First-Order Reliability Method

3.1.1. First-Order Reliability Method

The basic idea of the First-order reliability method (FORM) is to simplify the joint probability density function $f_x(x)$ and the approximate limit state function $g(x)$, primarily by performing a first-order Taylor approximation expansion at MPP [39–42]. The process of using FORM to calculate reliability includes coordinate space conversion and integral boundary approximation [43,44].

Coordinate space conversion refers to converting random variables subject to various probability distributions into variables subject to a standard normal distribution by the Rosenblatt method [45]. Suppose the random variable follows the normal distribution with mean value and standard deviation value, then the random variable transformed by the Rosenblatt method is

$$u = \frac{x - \mu}{\sigma}. \tag{8}$$

The approximation of the integral boundary is an important part of FORM. Its main idea is to perform first-order Taylor expansion of the integral boundary $g(u) = 0$ to make the integral solution of failure probability easier. The first-order Taylor expansion of $g(u)$ can be expressed as

$$g(u) = g(u^*) + \nabla g(u^*)(u - u^*)^T, \tag{9}$$

where u^* represents the expansion point; $\nabla g(u^*)$ represents the gradient of the expansion point. To reduce the precision loss caused by Taylor expansion, the MPP point on the fundamental boundary $g(u) = 0$ is expanded. Search for MPP points on integral boundary $g(u) = 0$, that is, maximize the joint probability density:

$$\begin{cases} \max & \prod_{i=1}^n \frac{1}{\sqrt{2\pi}} e^{-\frac{u_i^2}{2}} \\ \text{s.t.} & g(u) = 0 \end{cases}. \tag{10}$$

By observing Equation (10), it can be seen that the above process is a constrained optimization problem. The deformation of Equation (10) is carried out:

$$\prod_{i=1}^n \frac{1}{\sqrt{2\pi}} e^{-\frac{u_i^2}{2}} = \frac{1}{\sqrt{2\pi}} e^{-\frac{1}{2} \sum_{i=1}^n u_i^2}. \tag{11}$$

And,

$$\max \prod_{i=1}^n \frac{1}{\sqrt{2\pi}} e^{-\frac{u_i^2}{2}} \sim \min \sum_{i=1}^n u_i^2. \tag{12}$$

Therefore, the search model of MPP points can be expressed as:

$$\begin{cases} \min & \|u\| \\ \text{s.t.} & g(u) = 0' \end{cases} \tag{13}$$

where $\|u\| = \sqrt{u_1^2 + \dots + u_n^2}$ represents the magnitude of the vector u . The above formula is solved to obtain $u = u^*$, which is the MPP point. Let $\beta = \|u^*\|$, from the perspective of two-dimensional geometry, the MPP point can be viewed as the point $g(u) = 0$ tangent to a circle centered at the origin and with radius β . According to literature, the calculation formula of reliability can be expressed as:

$$R = \phi(\beta), \tag{14}$$

where $\phi(\cdot)$ represents the cumulative distribution function obeying normal distribution.

The above are the general steps of the First-order reliability analysis method. According to different solving methods, FORM can be divided into the Reliability Index Approach (RIA) [40] and the Performance Measure Approach (PMA) [46].

3.1.2. Reliability Index Method

RIA uses a reliability index instead of failure probability constraints, the mathematical model is the MPP point search model [47–50]. It can be seen that the mathematical model is an optimization problem. A variety of optimization algorithms, such as Sequential Quadratic Programming (SQP), can be used to solve the optimization model.

3.1.3. Performance Measure Approach

When the failure probability is 0 or 1, the corresponding reliability index will approach infinity or infinitesimal, resulting in RIA failure. At this time, PMA can be used to solve the problem. Its mathematical model is [51]:

$$\begin{cases} \min & g(u) \\ \text{s.t.} & \|u\| = \beta_t' \end{cases} \tag{15}$$

where β_t represents the target reliability index. The above model indicates that under the given reliability, if $g(u) > 0$, it means that the solution can meet the given reliability requirements.

Through the mathematical model of RIA and PMA, it can be seen that the solution of the two ways is a reciprocal inverse process. The difference is that the feasible region of PMA is a sphere, while that of RIA is a hypersurface. In terms of computational efficiency, PMA has more advantages than RIA.

3.1.4. Reliability Analysis Method Considering Stochastic and Interval Uncertainties

In the above introduction to FORM, design variables are random variables that obey a normal distribution. However, in many practical engineering applications, the distribution of some random variables may not be clear [52–54]. The possible values of these uncertain variables are usually only in the specified interval without accurate distribution information. That is, there is interval uncertainty. When dealing with such mixed uncertainty RBDO problems, the computational complexity will be greatly increased. A simple method is to treat the interval variables as random variables to approximate the calculation. Although this method can simplify the reliability analysis, it cannot guarantee the accuracy of the results [55]. To solve such problems, Du et al. [23] proposed a kind of mixed uncertainty analysis method.

Compared with the reliability analysis considering random and interval uncertainty, some changes should be made based on the original calculation model. The transformed RIA model is directly presented here:

$$\begin{cases} \min & \|u_{MPP}(y)\| \\ \text{s.t.} & g(u, y) = 0 \\ & y^L \leq y \leq y^U \end{cases} , \tag{16}$$

where y represents interval variable; y^L represents the lower bound of the interval; y^U is the upper bound of the interval. Similarly, the PMA mathematical model considering stochastic and interval uncertainty is:

$$\begin{cases} \min & g(d, u, y) \\ \text{s.t.} & \|u\| = \beta_t \\ & y^L \leq y \leq y^U \end{cases} \quad (17)$$

It can be seen that reliability analysis considering random and interval uncertainty is equivalent to adding a set of interval variables and changing the failure boundary based on reliability analysis considering random uncertainty. The rest parts are the same exactly. Therefore, when there is interval uncertainty, reliability analysis using the above method will not bring about redundant calculation steps, so it will not significantly reduce the calculation efficiency.

3.1.5. Method of Solving MPP Points by Improving PSO

For FORM, the main task is to solve the MPP points. According to the mathematical models of RIA and PMA, the solution of MPP points is an optimization problem with constraints. When solving optimization problems, intelligent optimization algorithms, including PSO, do not need gradient information [56–60]. They can deal with discrete variable optimization problems since they have strong global search ability [61,62]. The detailed steps of MPP point solving using the improved PSO algorithm are as follows.

When an intelligent optimization algorithm is used to solve MPP points, the probability constraint model in first-order reliability analysis can be processed by penalty function in general [63], as shown below:

$$\min f = \|U\| + \eta \max\{0, g(X)\}, \quad (18)$$

where f represents fitness; η represents the penalty factor, whose expression is:

$$\eta = \frac{100}{|g(\mu)|} \quad (19)$$

Taking fitness f as the optimization objective, the general steps of solving MPP points by using the improved PSO algorithm are shown as follows:

Step 1: Set the initial conditions for searching MPP points, including the limit state function $g(X)$, the probability distribution function of the design variable X (a normal distribution with mean value μ and standard deviation σ), parameters of PSO algorithm, namely: population number N , the total number of iterations ger , inertia coefficient w , and flight step length c ;

Step 2: Set the boundary conditions, including the lower bound $X^L = \mu - 5\sigma$ and upper bound $X^U = \mu + 5\sigma$ of the design variable; the maximum value $v_{\max} = X^U - X^L / 100$ and minimum value $v_{\min} = -v_{\max}$ of the speed;

Step 3: Generate the initial population. The initial position $X_0 = X^L + r \times (X^U - X^L)$ and initial velocity $V_0 = v_{\min} + r \times (v_{\max} - v_{\min})$ of the population should be calculated. The penalty factor η should be set;

Step 4: Update local optimal value p_{best} and global optimal value g_{best} . Firstly, the design variable U was converted into the random variable X , which obeyed the standard normal distribution. Then, fitness $f = \|U\| + \eta \max\{0, g(X)\}$ was calculated. Finally, p_{best} and g_{best} were screened out;

Step 5: Update the population location. The population location updating method mentioned above was used to update all the particles;

Step 6: Check whether convergence occurs. The convergence condition can be $g(g_{best}) < 0.001$ or $k = ger$. If either condition is satisfied, the iteration can be stopped and $X_{MPP} = g_{best}$ is output. Otherwise, do $k = k + 1$ and return to step (4) to continue the iteration.

The above is the method of solving MPP points by using the improved PSO.

3.2. The Used PSO Algorithm

By using the enhanced PSO algorithm, each constraint function is considered separately. During the algorithm process, the best fitness of each individual particle is updated through the constraint function, and then the best position of the particle is obtained by comparing the fitness of each individual. Through the optimal position of each particle in the population, the optimal population position for the current constraint function is finally obtained. Finally, by comparing the calculation results of each constraint function, the optimal MPP point is obtained. The calculation steps of the used PSO algorithm are shown in the Table 1.

Table 1. The calculation steps of the used PSO algorithm.

The PSO Algorithm	
Step 1	Firstly, PSO is used to generate a set of initial solutions;
Step 2	For each particle, the value of its objective function is calculated and the current optimal solution is recorded;
Step 3	Calculate the speed of each particle, according to the speed of updating the positions of the particles in the solution space;
Step 4	Using the Metropolis criterion to decide whether to accept the new position;
Step 5	The particles are updated in a certain order to make the local optimal particle position move to the global optimal, which improves the global search performance of the algorithm
Step 6	Repeat Steps 2 through 5 until the termination condition is reached

By using this method, the advantages of a simple and efficient PSO algorithm can be brought into play. The SA algorithm can keep the original performance without expending the energy to adjust the parameters.

3.3. RBDO Decoupling Method

RBDO solution strategies can be divided into double-loop method, single-loop method, and decoupling method [64]. The double-loop method is the most basic and direct solution strategy [65]. Its flow is a double-layer nested cycle optimization flow. What is more, its solving efficiency is the lowest. The single-loop method is the most efficient solution strategy. However, it has problems such as low precision and difficult convergence [66]. Compared with the other two methods, the decoupling strategy is a very important RBDO method, which can give consideration to both solving accuracy and solving efficiency.

Sequence Optimization and Reliability Assessment (SORA) method is an efficient decoupling method for solving RBDO problems [67]. Based on the decoupling idea, SORA serializes the traditional two-layer nested cycle optimization process. Forming a sequential deterministic design optimization and controllability analysis process [68]. The main idea of SORA is to approximate the solution of the RBDO problem. The main method is to make the constraint gradually shift to the direction of the probability constraint, so as to quickly get the optimal solution. Its mathematical expression is

$$\begin{cases} \text{find : } & \mu_X \\ \text{min : } & C(\mu_X) \\ \text{s.t. } & g_i(\mu_X - s_i) \geq 0 (i = 1, 2, \dots, m) \\ & \mu_X^L \leq \mu_X \leq \mu_X^U \end{cases} \quad (20)$$

where $s_i = \mu_X^{(k-1)} - x_i^*$ ($i = 1, 2, \dots, m$) is the offset vector of the i th probability constraint; 3 was the design point of the last iteration. In SORA, each iteration cycle will construct an offset vector based on the reliability analysis results of the previous iteration to move the boundary of the probability constraint. According to the constraint boundary after

moving, the DO is constructed to update the optimal design scheme. The nested RBDO is decomposed into a series of reliability analyses and DO problems.

3.4. The Proposed RBDO Method Based on the PSO and SA Algorithm

The analysis optimization method proposed in this paper is a fusion of the meta-heuristic algorithm RBDO method. Its main idea is that: the SA algorithm and enhanced PSO algorithm are, respectively, used to perform reliability optimization and reliability analysis after decoupling. The purpose of improving the efficiency of analysis and optimization is achieved.

The overall process is as follows:

- Step 1: Set the probability distribution of random variables and the reliability index of the target β_t ;
- Step 2: Set parameters of the PSO algorithm and SA algorithm;
- Step 3: Enter the optimization cycle of the SA algorithm. Select the design variable set in step (1) as the initial point to calculate the value of the objective function;
- Step 4: Reliability analysis is carried out on the results obtained in step (3). The improved PSO algorithm is used to solve the MPP points, calculate the reliability index, and judge its reliability. If the reliability requirements are met, this solution is output as the optimal solution. Otherwise, calculate the offset vector, update the probability constraint function, and return to step (3) for a new round of reliability optimization.

The pseudocode is shown below:

```

Set initial variables
While1 Reliability index not met
  %%Obtain the optimal solution space through annealing method
  Using simulated annealing method to generate initial solution space
  Random number generator initialization
  While2 Does not meet Metropolis criterion Equation (7)
    For From 1 to the set number of annealing times
      Generate random perturbations to obtain new solutions
      Check whether the Metropolis criterion Equation (7) is met, if so, exit the
current annealing
      Perform annealing and save the optimal solution during the annealing process.
    End for loop
    Update random number generator
  End the while2 loop and obtain the optimal design variable solution space
  %%Using PSO algorithm to find MPP points
  %%Perform the following operations for each limit state function
  Initialize the population position and velocity according to the optimal solution space
obtained by the annealing algorithm
  While3 The current iteration is less than the maximum number of iterations
    Update the population position and velocity according to the objective function value of
each population particle
    Dealing with boundary issues
  End the current while3 loop
  Translational failure boundary
  Solve to obtain the optimal MPP point
  Use this point as the initial solution space for the next cycle.
End the while1 loop
    
```

The flowchart of this method is shown in Figure 2:

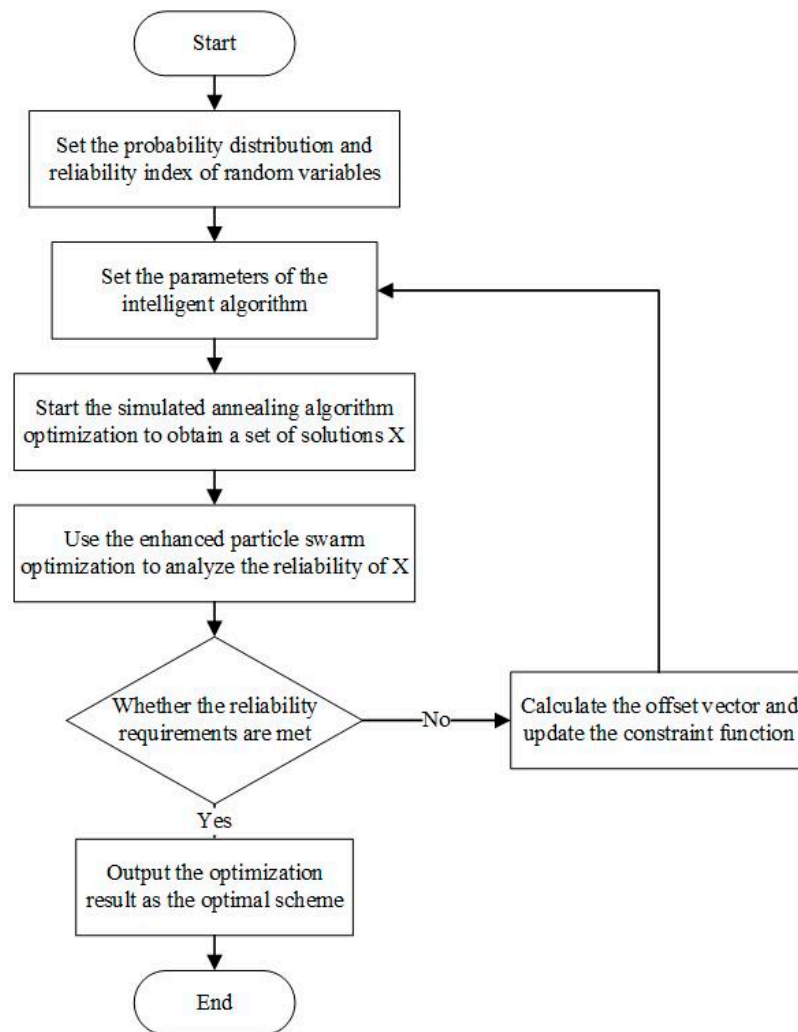


Figure 2. Flow chart of RBDO algorithm incorporating meta-heuristic algorithm.

4. Experimental Results and Discussion

4.1. Example Verification

In order to obtain the performance of reliability analysis by using the PSO algorithm, two mathematical examples are selected in this section for verification. The SQP method and Monte Carlo Simulation (MCS) are selected as a comparison. The MCS is considered an approximate solution. Therefore, its calculation error is considered to be 0. In this article, it is represented by the symbol “—”. The two examples are a convex function and a concave function, respectively. The variables of the convex function only have random uncertainty, while those of the concave function have both random uncertainty and interval uncertainty.

4.1.1. Convex Limit State Function

The expression of the limit state function of this example is:

$$g = -e^{x_1-7} - x_2 + 10, \tag{21}$$

where both x_1 and x_2 have random uncertainty; $x_1 \sim N(6.0, 0.8), x_2 \sim N(6, 0.8)$. The limit state function is solved. Its convergence process is shown in Figure 3. Different colors in the figure represent contour distribution. The red dot represents the optimization solution process. The comparison of results is shown in Table 2 below:

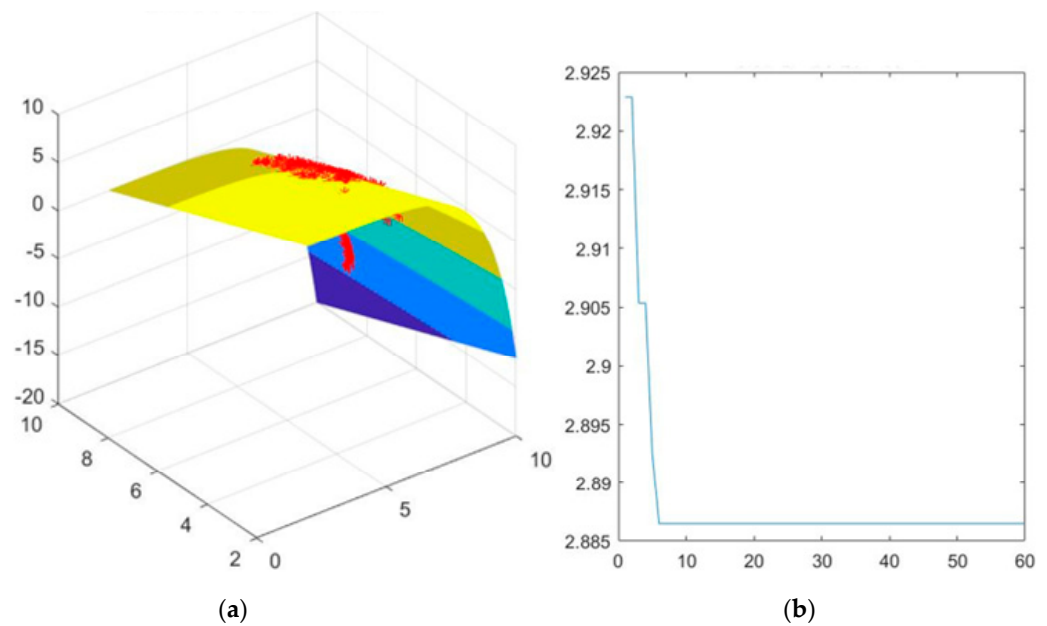


Figure 3. Convex function iterative solution procedure. (a) State position change—Number of iterations: 60 (b) Optimal fitness evolution process.

Table 2. Reliability index of the convex function.

Method	Reliability Index	Error	Solution Time (Milliseconds)
MCS	2.8445	—	1,948,731.39
SQP	2.8782	1.2%	988.71
Improved PSO	2.8865	1.5%	47.67

It can be seen from the calculation results that the improved PSO algorithm is equivalent to the SQP algorithm in solving accuracy. However, about 50% faster than the SQP algorithm. It can be seen that the PSO algorithm has better performance in reliability analysis under stochastic uncertainty.

4.1.2. Concave Limit State Function

In this example, the limit state function can be expressed as:

$$g = \frac{e^{0.8x_1-1.2} + e^{0.7x_2-0.6} - 7}{10}, \tag{22}$$

where variable x_1 has random uncertainty, $x_1 \sim N(4.0, 0.8)$; variable x_2 has interval uncertainty, $x_2 \in [3.2, 4.2]$. To solve this concave limit state function, the convergence process is shown in Figure 4. Different colors in the figure represent contour distribution. The red dot represents the optimization solution process. The comparison of results is shown in Table 3.

It can be seen from the table that the accuracy of PSO is about 24% higher than that of SQP when solving the concave limit state function considering random and interval uncertainty. It can be seen that the sequential quadratic programming algorithm is not suitable for dealing with the reliability analysis problem of concave functions under mixed uncertainty. The improved PSO algorithm has good fitness when dealing with the mixed uncertainty analysis problems of convex function type and concave function type, which proves that the performance of the PSO algorithm is good enough to solve MPP points in first-order reliability analysis.

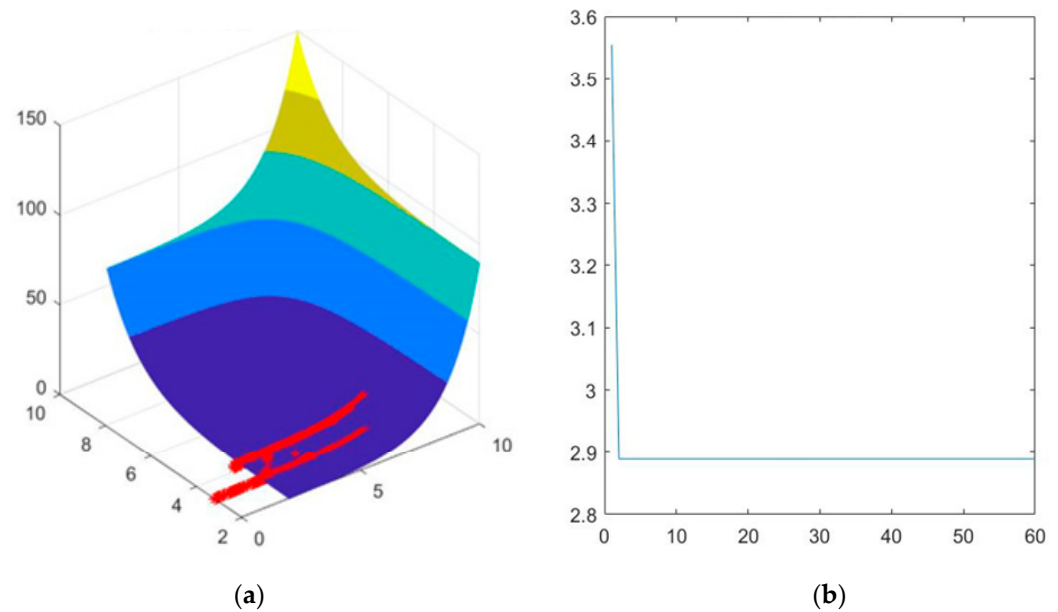


Figure 4. Concave function iterative solution procedure. (a) State position change-Number of iterations: 60 (b) Optimal fitness evolution process.

Table 3. Concave function reliability index.

Method	Reliability Index	Error	Solution Time (Milliseconds)
MCS	2.9906	--	1,851,997.89
SQP	2.1681	27.5%	80.32
Improved PSO	2.8891	3.4%	228.12

4.2. Mathematical Example

In this section, a nonlinear mathematical example is used to verify the RBDO method of the proposed fusion meta-heuristic algorithm. The objective function of this mathematical example is the sum of two normally distributed design variables x_1 and x_2 . The constraint function consists of three nonlinear functions. The mathematical model of the optimization problem is as follows:

$$\begin{cases} \text{find } \mu_X = [\mu_{x_1}, \mu_{x_2}] \\ \text{min } f(\mu_x) = \mu_{x_1} + \mu_{x_2} \\ \text{s.t. } Prob(g_i(X) \geq 0) \geq \varphi(\beta^t), i = 1, 2, 3 \end{cases}, \tag{23}$$

where β^t represents the target reliability index. Its value here is $\beta^t = 3.0$; μ_{x_1} and μ_{x_2} are the mean values of design variables x_1 and x_2 , respectively. Their standard deviation σ is 0.3. The mean values range between 0 and 10, i.e.,:

$$\begin{cases} X \sim N(\mu_X, 0.3^2) \\ 0 \leq \mu_X \leq 10 \end{cases} \tag{24}$$

The limiting equation of state is

$$\begin{cases} g_1(X) = x_1^2 x_2 / 20 - 1 \\ g_2(X) = (x_1 + x_2 - 5)^2 / 30 + (x_1 - x_2 - 12)^2 / 120 - 1 \\ g_3(X) = 80 / (x_1^2 + 8x_2 + 5) - 1 \end{cases} . \tag{25}$$

The solution space formed by the limit state equation is shown in Figure 5.

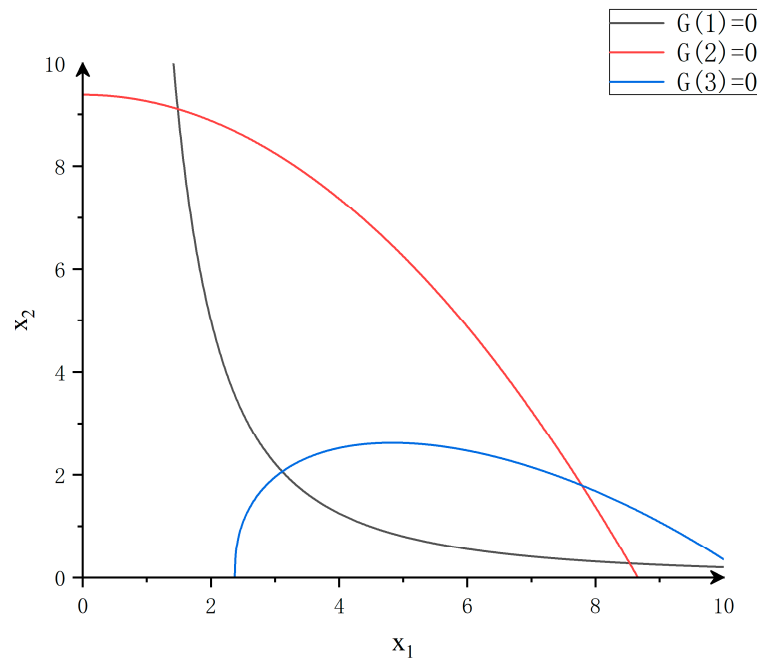


Figure 5. Design variable feasible domain.

In order to test the performance of the RBDO method of the fusion meta-heuristic algorithm proposed in this paper, the proposed method is compared with the results obtained by using the optimization algorithm SQP, GA, and the theoretical solution in the literature [69]. The results are shown in Table 4. “--” means there is no relevant information in Table 4.

Table 4. Optimization result.

Method	Optimal Solution	Error	Solution Time (Milliseconds)
Theoretical method	6.7318	--	--
SQP	7.4195	10.2%	320.5
GA	6.9754	3.6%	6975.4
The proposed method	7.0988	5.5%	211.9

As shown in Table 4, the method proposed in this study is identical to the results obtained using two other heuristic algorithms SQP and Genetic algorithm (GA). Compared with SQP method, the method proposed in this study is closer to the exact solution. Compared with GA method, the time used in this study is greatly reduced, and the solving speed is increased by 32 times. It can be seen that the method proposed in this study has reliable accuracy and superior solving efficiency.

4.3. Volume Optimization of Gear Reducer

In the engineering example of this section, a classic case of the gear reducer is selected to optimize the reliability design. In order to verify the method presented in this paper [70,71], the original example is modified to make it a single-discipline design optimization problem considering stochastic and interval uncertainty.

The structure diagram of the gear reducer is shown in Figure 6. The optimization model has seven design variables that determine the component size of the reducer. When only random uncertainty analysis is considered, all seven variables are set as random variables and have a normal distribution, as shown in Table 5. At the same time, this study also considers mixed random variables to improve the accuracy of calculation results. As shown in Table 6, change the diameter of the axis to an interval variable. In this example, the target reliability index is set as $\beta_t = 2.4$. The corresponding reliability is $R = 99.18\%$.

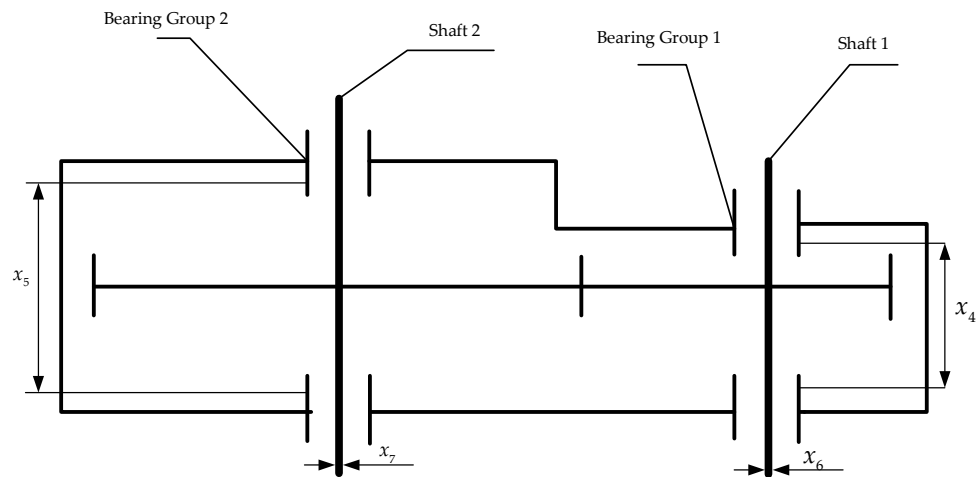


Figure 6. Structure diagram of gear reducer.

Table 5. Random uncertainty description.

Design Variable	Mean Value	Standard Deviation	Distribution Type	Lower Bound of Mean	Upper Bound of Mean
Tooth width factor x_1	x_1^M	$0.01x_1^M$	Orthographic distribution	2.63	3.57
Module of gear teeth x_2	x_2^M	$0.01x_2^M$	Orthographic distribution	0.71	0.81
Number of teeth of gear 1 x_3	x_3^M	$0.01x_3^M$	Orthographic distribution	17	23
Length of shaft 1 x_4	x_4^M	$0.01x_4^M$	Orthographic distribution	7.31	8.29
Length of shaft 2 x_5	x_5^M	$0.01x_5^M$	Orthographic distribution	7.31	8.29
Shaft 1 diameter x_6	x_6^M	$0.01x_6^M$	Orthographic distribution	2.93	3.87
Shaft 2 diameter x_7	x_7^M	$0.01x_7^M$	Orthographic distribution	5.03	5.47

Table 6. Interval uncertainty description.

Design Variable	Upper Bound of Interval	Lower Bound of Interval
Shaft 1 diameter x_6	2.93	3.87
Shaft 1 diameter x_7	5.03	5.47

In this optimization problem, the objective is to minimize the volume V of the gear reducer, whose mathematical expression is

$$V = V_1 + V_2, \tag{26}$$

where V_1 and V_2 represent the volume of the gear and the volume of the bearing, respectively. The volume of the gear can be expressed as

$$V_1 = 0.7854x_1x_2^2(3.3333x_3^2 + 14.9334x_3 - 43.0934) - 1.508x_1(x_6^2 + x_7^2). \tag{27}$$

The volume of the bearing can be expressed as

$$V_2 = 7.477(x_6^3 + x_7^3) + 0.7854(x_4x_6^2 + x_5x_7^2). \tag{28}$$

The constraint function is the related performance index of the gear reducer, including stress, size, displacement, etc., 11 in total.

The optimization model of this problem is

$$\begin{cases} \text{find } X = [x_1, x_2, x_3, x_4, x_5, x_6, x_7] \\ \text{min } f = V_1 + V_2 \\ \text{s.t. } Prob(g_i(X) \geq 0) \geq \varphi(\beta^t), i = 1, 2, \dots, 11 \end{cases} \quad (29)$$

The stress constraint function of the gear reducer performance is

$$\begin{cases} g_1 = 1 - 27/(x_1x_2^2x_3) \\ g_2 = 1 - 397.5/(x_1x_2^2x_3^2) \\ g_3 = 12 - x_1/x_2 \\ g_4 = x_1/x_2 - 5 \end{cases} \quad (30)$$

The dimension constraint function is

$$\begin{cases} g_5 = 1 - 1.93x_4^3/(x_2x_3x_6^4) \\ g_6 = 1 - 1.93x_5^3/(x_2x_3x_7^4) \\ g_7 = 1100 - A_1/B_1 \\ g_8 = 1 - (1.5x_6 + 1.9)/x_4 \\ g_9 = 1 - (1.1x_7 + 1.9)/x_5 \end{cases} \quad (31)$$

where $A_1 = \sqrt{[745x_4/(x_2x_3)]^2 + 16.9 \times 10^6}$; $B_1 = 0.1x_6^3$.

The displacement constraint function is

$$\begin{cases} g_{10} = 850 - A_2/B_2 \\ g_{11} = 40 - x_2x_3 \end{cases} \quad (32)$$

where $A_2 = \sqrt{[745x_5/(x_2x_3)]^2 + 157.5 \times 10^6}$, $B_2 = 0.1x_7^3$.

For this optimization model, the RBDO method of fusion meta-heuristic algorithm proposed in this paper is used to solve it. Meanwhile, the case where only random uncertainty is considered is calculated. The calculation results of the two uncertain cases are shown in Table 7 below.

Table 7. Optimization result.

Uncertainty Description	Optimal Solution	Error
Comparison method(MCS)	2753.8	
SQP	2851.2653	3.54%
GA	2891.1236	4.99%
The proposed method 1	2773.0126	0.69%
The proposed method 2	2814.9546	2.22%

For this algorithm, this study uses the results obtained by MCS to be approximately regarded as the exact solution to compare other solutions. Judging from the calculation results in Table 7, it is found that when using the optimization results (The proposed method 1) that do not consider mixed variables, the optimization results of this article are very close to the exact solution. Considering the complex influencing factors in engineering, this paper also adopts complex optimization conditions that consider multiple variables. Although the result is worse than the proposed method 1, it has higher stability. In addition, this article also compared it with two other heuristic algorithms, SQP and GA algorithms, and found that the results of this algorithm are basically consistent with the other two results. This proves the feasibility of this method.

4.4. Composite Cylinder Size Optimization

This section further illustrates the effectiveness of the proposed method by combining cylinder size optimization cases [72]. The composite cylinder is composed of an inner cylinder and an outer cylinder. The inner diameter of the inner cylinder is a , the outer diameter is b , the inner diameter of the outer cylinder is b , and the outer diameter is c . The height of the composite cylinder is 50 mm. The cylinder body is subjected to a pressure of size p . The structure and initial size of the composite cylinder are shown in Figure 7.

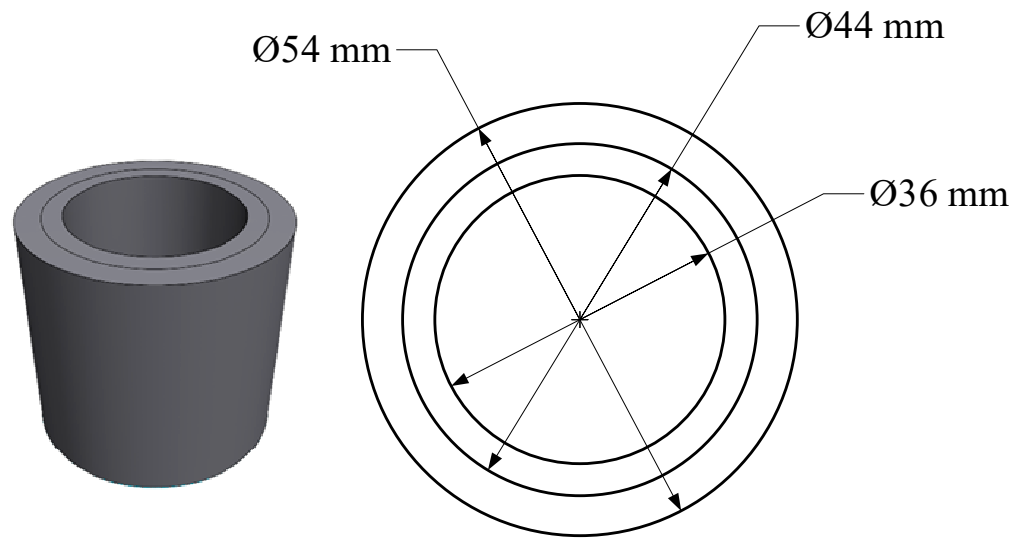


Figure 7. Composite cylinder structure diagram.

The optimization goal of the composite cylinder is to minimize the volume of the composite cylinder while satisfying the allowable equivalent stress and tangential stress of the inner and outer cylinders. The optimization problem includes three design variables: x_1 , x_2 , and x_3 , corresponding to the inner diameter a and outer diameter b of the inner cylinder and the outer diameter c of the outer cylinder, respectively. There are 8 constraint conditions, among which the equivalent stress and tangential stress are all implicit expressions. The approximate mathematical expressions need to be established by finite element analysis. The optimization model of the composite cylinder is as follows:

$$\begin{cases} \text{find} & x = (x_1, x_2, x_3) \\ \text{max} & f = V = 12.5\pi x_1^2 \\ \text{s.t.} & \text{Prob}(g_i(X) \geq 0) \geq \varphi(\beta^t), i = 1, 2, \dots, 8 \end{cases}, \tag{33}$$

where β^t is the target reliability index. Here, $\beta^t = 2.4$.

The stress constraint and geometric constraint of the inner cylinder are

$$\begin{cases} g_1 = S - S_1 \\ g_2 = \tau - \tau_1^a \\ g_3 = \tau - \tau_1^b \\ g_4 = b - 1.2a \end{cases}. \tag{34}$$

The stress constraint and geometric constraint of the outer cylinder are

$$\begin{cases} g_5 = S - S_2 \\ g_6 = \tau - \tau_2^b \\ g_7 = \tau - \tau_2^c \\ g_8 = c - 1.2b \end{cases}. \tag{35}$$

The value range of the design variable of the composite cylinder is as follows:

$$\begin{cases} 31.496 \leq a \leq 40.64 \\ 38.1 \leq b \leq 50.8 \\ 30.48 \leq c \leq 60.96 \end{cases}, \tag{36}$$

where S and τ represent allowable equivalent stress and tangential stress, respectively; S_1 and S_2 represent the maximum equivalent stress of inner cylinder and outer cylinder, respectively; τ_1^a and τ_1^b represent the maximum tangential stress on inside diameter a and outside diameter b of the inner cylinder; τ_2^b and τ_2^c represent the maximum tangential stresses on inside diameters b and outside diameters c of the outer cylinder. Ansys Workbench software was used for finite element analysis. The relevant parameters of the composite cylinder are shown in Table 8.

Table 8. Composite cylinder-related parameters.

Name	Symbol	Value
Modulus of elasticity/GPa	E	210
Poisson’s ratio	ρ	0.3
Internal pressure/MPa	p	139.7
Allowable stress/MPa	S	607.7
Allowable shear stress/MPa	τ	244.5

Three-dimensional modeling was carried out in Ansys Workbench. The inner diameter a of the inner cylinder, outer diameter b of the inner cylinder, and outer diameter c of the outer cylinder were set as input parameters, which were used to solve the subsequent response surface. Tetrahedral elements are used to divide the grid. To ensure the number of elements and nodes on the composite cylinder wall, the cell size is set as 1 mm. The displacement constraints in the direction of X, Y, and Z are, respectively applied to the cylinder end face of the composite cylinder. Meanwhile, the stress loading p is applied to the inner cylinder of the inner cylinder. The contact between the inner cylinder and the inner cylinder is selected as “no separation” in the “connection” option. The equivalent stress and maximum shear stress were solved, respectively. The results are shown in Figure 8. The equivalent stress and maximum shear stress were set as output parameters.

According to the results of finite element analysis, the stress of the inner cylinder exceeds the maximum allowable value, so it cannot meet the use requirements at present. Its size parameters need to be further optimized. In this example, the expressions of the equivalent stress and tangential stress are approximated by polynomials. Quadratic polynomials with cross terms are selected here. The form is that the finite element analysis results show that the stress of the inner cylinder exceeds the maximum allowable value, so it cannot meet the use requirements at present. Its size parameters need to be further optimized. In this example, the expressions of equivalent stress and tangential stress are approximated by polynomials. Here, the quadratic polynomial with cross terms is selected. Its form is

$$\tilde{F}(x) = a_0 + \sum_{i=1}^3 b_i x_i + \sum_{i=1}^3 c_i x_i^2 + \sum_{i=1}^2 \sum_{j=i+1}^3 d_{ij} x_i x_j + e_{123} x_1 x_2 x_3. \tag{37}$$

The response surface module in Ansys Workbench software is used to generate design points and calculate corresponding output values. The results are shown in Table 9.

The coefficients of the quadratic polynomial are solved in Matlab by using the above 10 groups of design points. The obtained values of each system are shown in Table 10.

By the above method, the limit state function is expressed explicitly instead of implicitly. In this problem, which has random uncertainty, their probability distribution is normal. Their standard deviation is 1% of their mean. c has interval uncertainty. Its value range is

shown in Equation (36). The results are shown in Table 11 below. It can be seen from the optimization results that the method proposed in this article can obtain a smaller objective function value. This shows that the optimization results obtained by this method are more superior. In order to verify the feasibility of this method, the optimization results of this method are modeled and analyzed through finite element analysis.

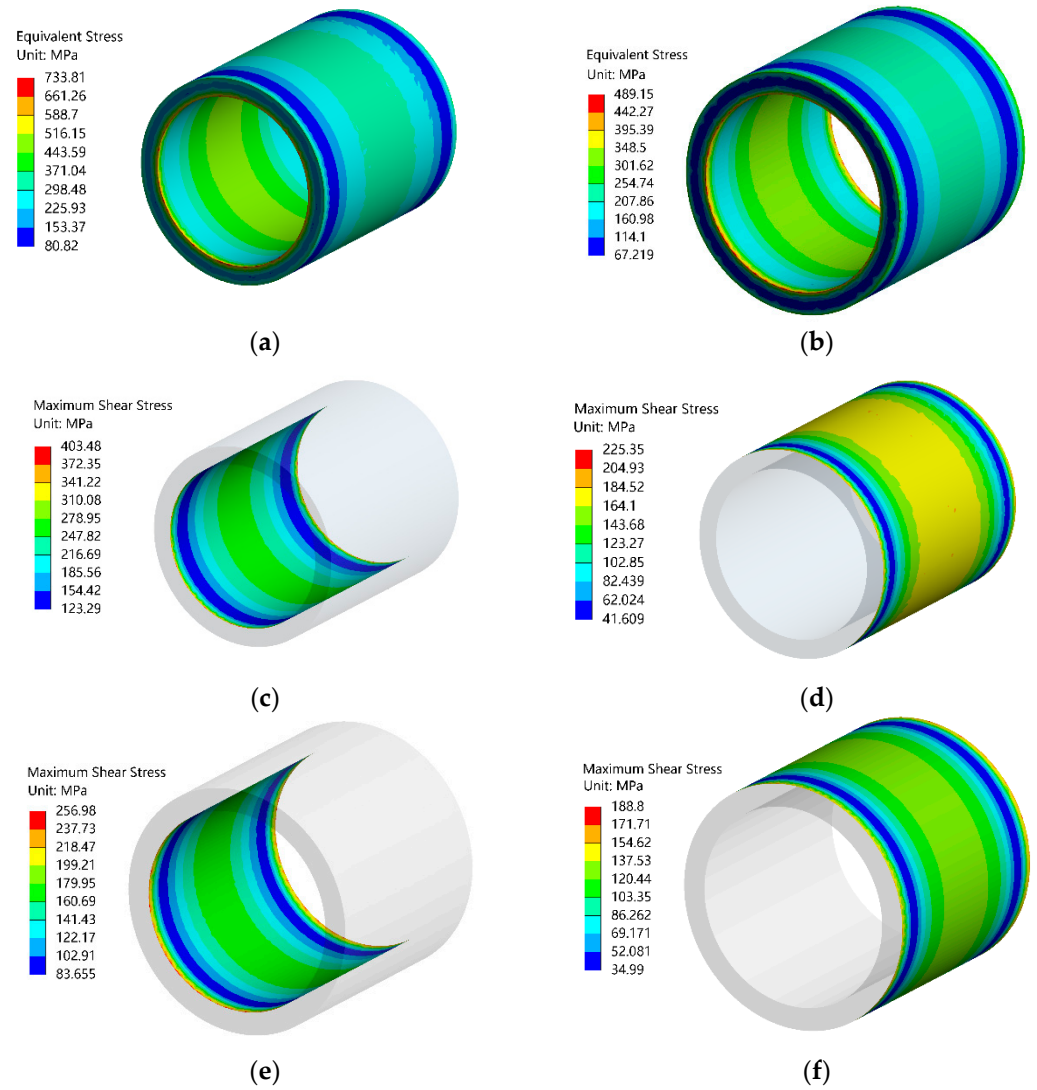


Figure 8. Stress nephogram of the composite cylinder. (a) Equivalent stress of inner cylinder, (b) Equivalent stress of outer cylinder, (c) Tangential stress on inner diameter of the inner cylinder, (d) Tangential stress on outer diameter of the inner cylinder, (e) Tangential stress on inner diameter of the outer cylinder, and (f) Tangential stress on the outer diameter of the outer cylinder.

Table 9. Design point.

	<i>a</i>	<i>b</i>	<i>c</i>	<i>S</i> ₁	<i>S</i> ₂	τ_1^a	τ_1^b	τ_2^b	τ_2^c
1	38.5	39.9	49.7	889.90	997.82	483.00	400.66	526.84	346.94
2	39.2	49.6	53.1	1069.30	518.25	578.87	273.39	273.69	180.97
3	33.0	49.5	55.5	589.82	252.57	324.35	130.22	133.18	89.94
4	39.3	43.8	58.0	792.55	528.81	441.83	281.42	279.47	186.87
5	37.1	47.6	50.4	751.12	438.64	414.24	234.62	230.51	177.81
6	32.8	39.7	52.7	605.15	391.49	337.28	195.88	207.00	135.23
7	34.2	43.1	52.3	811.37	436.74	442.53	218.96	231.57	170.05
8	36.4	49.0	56.8	881.32	430.42	483.57	201.98	226.71	155.63

Table 9. Cont.

	<i>a</i>	<i>b</i>	<i>c</i>	S_1	S_2	τ_1^a	τ_1^b	τ_2^b	τ_2^c
9	39.7	47.5	49.7	1256.80	565.43	675.41	353.23	308.07	260.49
10	39.7	49.5	55.1	990.28	564.01	536.79	274.83	297.29	199.18

Table 10. Polynomial coefficient.

	S_1	S_2	τ_1^a	τ_1^b	τ_2^b	τ_2^c
a_0	1,306,319	41,973.2	685,669.2	116,143.7	34,266.6	−23,063.3
b_1	−34,404	−644.3	−18,032.3	−2974.9	−663.4	748.8
b_2	−28,761.7	−1219.7	−15,093.5	−2522.8	−894.6	502.7
b_3	−24,292.4	−753.5	−12,764.2	−2184.7	−628.1	367.9
c_1	−5	−1.7	−3	0.8	−0.7	0.6
c_2	−10.9	0.5	−5.5	−1.1	0.01	−1.7
c_3	−9.4	−3.1	−4.7	−0.4	−1.5	0.3
d_{12}	761.1	18.5	399.3	65.2	16.7	−14
d_{13}	645.8	18.3	339	55.2	15.2	−14.6
d_{23}	550.9	23.7	288.7	48.9	17.5	−6.8
e_{123}	−14.1	−0.4	−7.4	−1.2	−0.3	0.3

Table 11. Optimization result.

Variable	<i>a</i>	<i>b</i>	<i>c</i>	<i>V</i>
GA	37.65	38.10	59.58	55,662.18
SQP	38.47	38.10	59.26	57,190.73
Result	37.40	45.72	60.96	54,929.13

In order to verify the accuracy of the results, modeling and finite element analysis were conducted on the optimized composite cylinder again. The results are shown in Figure 9. It can be seen from the stress program that the maximum equivalent stress and maximum shear stress of the composite cylinder do not exceed the allowable value, which proves that the optimization scheme is feasible.

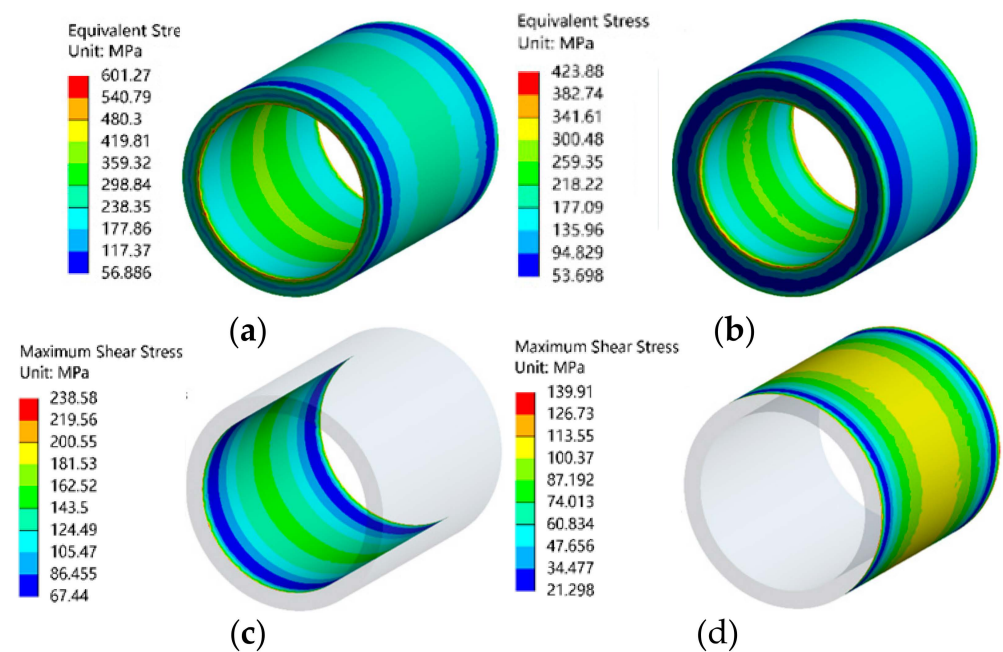


Figure 9. Cont.

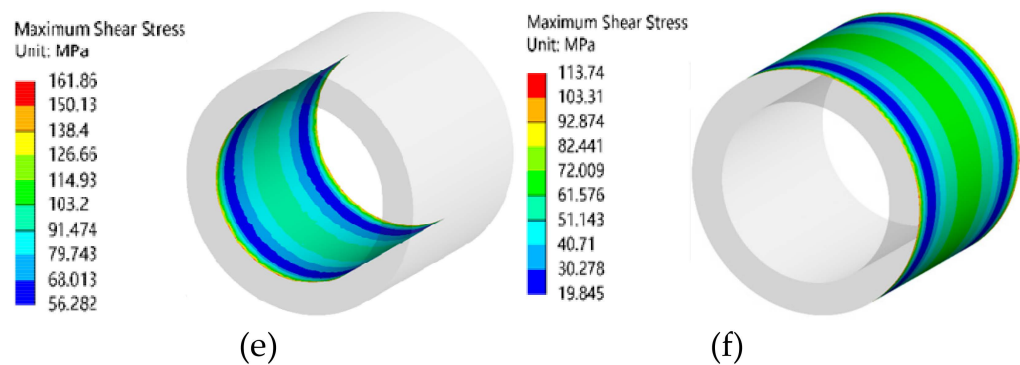


Figure 9. Stress nephogram of the composite cylinder after optimization. (a) Equivalent stress of inner cylinder, (b) Equivalent stress of outer cylinder, (c) Tangential stress on inner diameter of the inner cylinder, (d) Tangential stress on outer diameter of the inner cylinder, (e) Tangential stress on inner diameter of the outer cylinder, and (f) Tangential stress on the outer diameter of the outer cylinder.

5. Conclusions

This study constructs a RBDO method framework for RBDO considering mixed uncertainties, combined with a metaheuristic algorithm with superior performance. The research contents include: (1). Through the enhanced PSO algorithm, give full play to the global optimization ability of the algorithm to obtain better MPP points for the update optimization of the SA algorithm; (2). Through the decoupling method, the enhanced PSO of the algorithm is combined with the SA algorithm and put into an optimization framework. Realize the construction of a complete reliability-based design optimization algorithm; (3). Adopt a decoupling optimization strategy based on the SA algorithm, taking advantage of the faster convergence characteristics of SA. Compared with the ordinary double-loop method and single-loop method, this optimization method has faster solution efficiency and solution accuracy. The method proposed in this paper is dedicated to solving the RBDO problem considering mixed uncertainties. By applying the metaheuristic algorithm to the reliability analysis and optimization process of engineering structures, it provides new ideas to solve the problems of high computational cost and slow solution efficiency during the design optimization of increasingly complex engineering structures. Through the improved PSO algorithm and the decoupled convergence process combined with the SA algorithm, on the basis of ensuring the accuracy of the convergence results, the optimization efficiency is improved and the problem of easily falling into local convergence is solved. At the end of the article, the feasibility and superiority of this method are verified through a mathematical example and two complex engineering examples. It can be seen from the optimization results that compared with the double-loop RBDO method using the SQP method and the ordinary reliability optimization based on the first-order Taylor formula, the results of this method are better and the calculation efficiency is higher. Through the finite element analysis of the results and combined with the constraint conditions, it was found that under the same load conditions, the results of this method have smaller deformation amounts and stress and strain values. The reliability and feasibility of this method are proved.

In order to synthesize the role of each constraint function and obtain the optimal MPP point, this study performed equal calculations on each constraint function. However, in actual engineering, different constraint functions play different roles for each engineering situation, and sometimes there are even situations where the function does not play a constraining role. Therefore, in future work, by reducing the calculation of ineffective constraint functions in RBDO, the efficiency of optimization calculations can be further greatly improved.

This study uses the improved PSO algorithm to solve the global optimal MPP point, although it is compared with the SQP method and the simple FORM method. However, heuristic algorithms include more, such as multi-objective flower pollination algorithm,

multi-objective bat algorithm, multi-objective multiverse optimization, and multi-objective water cycle optimizer algorithms that are not mentioned in the article. In future work, it will be meaningful to explore and compare the efficiency of various optimization algorithms in solving RBDO problems considering mixed uncertainties.

Author Contributions: Conceptualization, S.Y., H.W., Y.X., Y.G., L.P., J.Z., X.G., D.M. and J.W.; Methodology, S.Y., H.W., Y.X., Y.G., L.P., J.Z., X.G., D.M. and J.W.; Validation, S.Y., H.W., Y.X., Y.G., L.P., J.Z., X.G., D.M. and J.W.; Formal analysis, S.Y., H.W., Y.X., Y.G., L.P., J.Z., X.G., D.M. and J.W.; Resources, S.Y., H.W., Y.X., Y.G., L.P., J.Z., X.G., D.M. and J.W.; Writing—original draft, S.Y., H.W., Y.X., Y.G., L.P., J.Z., X.G., D.M. and J.W.; Writing—review and editing, S.Y., H.W., Y.X., Y.G., L.P., J.Z., X.G., D.M. and J.W.; Funding acquisition, Y.X., Y.G., L.P., J.Z., X.G. and D.M. All authors have read and agreed to the published version of the manuscript.

Funding: This research was funded by the National Natural Science Foundation of China (Grant No. 52175130), the Guangdong Basic and Applied Basic Research Foundation (Grant No. 2022A1515240010), the Sichuan Science and Technology Program (Grants No. 2022YFQ0087 and 2022JDJQ0024), and Students Go Abroad for Scientific Research and Internship Funding Program of University of Electronic Science and Technology of China.

Data Availability Statement: All data that support the findings of this study are included within the article.

Conflicts of Interest: Authors Yongqiang Guo, Lidong Pan, and Jiaming Zhang were employed by the company Beijing Research Institute of Mechanical & Electrical Technology Ltd. The remaining authors declare that the research was conducted in the absence of any commercial or financial relationships that could be construed as a potential conflict of interest.

References

1. Zhong, Y.; Chen, Z.; Zhou, Z.; Hu, H. Uncertainty analysis and resource allocation in construction project management. *Eng. Manag. J.* **2018**, *30*, 293–305. [[CrossRef](#)]
2. Zhu, Q. Nonlinear Systems: Dynamics, Control, Optimization and Applications to the Science and Engineering. *Mathematics* **2022**, *10*, 4837. [[CrossRef](#)]
3. Meng, D.; Yang, S.; He, C.; Wang, H.; Lv, Z.; Guo, Y.; Nie, P. Multidisciplinary design optimization of engineering systems under uncertainty: A review. *Int. J. Struct. Integr.* **2022**, *13*, 565–593. [[CrossRef](#)]
4. Tan, Y.; Zhan, C.; Pi, Y.; Zhang, C.; Song, J.; Chen, Y.; Golmohammadi, A.M. A Hybrid Algorithm Based on Social Engineering and Artificial Neural Network for Fault Warning Detection in Hydraulic Turbines. *Mathematics* **2023**, *11*, 2274. [[CrossRef](#)]
5. Xue, Y.; Deng, Y. Extending set measures to orthopair fuzzy sets. *Int. J. Uncertain. Fuzziness Knowl.-Based Syst.* **2022**, *30*, 63–91. [[CrossRef](#)]
6. Zhu, S.P.; Keshtegar, B.; Bagheri, M.; Hao, P.; Trung, N.T. Novel hybrid robust method for uncertain reliability analysis using finite conjugate map. *Comput. Methods Appl. Mech. Eng.* **2020**, *371*, 113309. [[CrossRef](#)]
7. Bagheri, M.; Zhu, S.P.; Ben Seghier, M.E.A.; Keshtegar, B.; Trung, N.T. Hybrid intelligent method for fuzzy reliability analysis of corroded X100 steel pipelines. *Eng. Comput.* **2021**, *37*, 2559–2573. [[CrossRef](#)]
8. Plotnikov, L. Preparation and Analysis of Experimental Findings on the Thermal and Mechanical Characteristics of Pulsating Gas Flows in the Intake System of a Piston Engine for Modelling and Machine Learning. *Mathematics* **2023**, *11*, 1967. [[CrossRef](#)]
9. Zhang, D.; Zhang, J.; Yang, M.; Wang, R.; Wu, Z. An enhanced finite step length method for structural reliability analysis and reliability-based design optimization. *Struct. Multidiscip. Optim.* **2022**, *65*, 231. [[CrossRef](#)]
10. Meng, D.; Yang, S.; De Jesus, A.M.; Fazerer-Ferradosa, T.; Zhu, S.P. A novel hybrid adaptive Kriging and water cycle algorithm for reliability-based design and optimization strategy: Application in offshore wind turbine monopile. *Comput. Methods Appl. Mech. Eng.* **2023**, *412*, 116083. [[CrossRef](#)]
11. Yang, I.T.; Hsieh, Y.H. Reliability-based design optimization with discrete design variables and non-smooth performance functions: AB-PSO algorithm. *Autom. Constr.* **2011**, *20*, 610–619. [[CrossRef](#)]
12. Yang, M.; Zhang, D.; Wang, F.; Han, X. Efficient local adaptive Kriging approximation method with single-loop strategy for reliability-based design optimization. *Comput. Methods Appl. Mech. Eng.* **2022**, *390*, 114462. [[CrossRef](#)]
13. Meng, Z.; Li, G.; Wang, B.P.; Hao, P. A hybrid chaos control approach of the performance measure functions for reliability-based design optimization. *Comput. Struct.* **2015**, *146*, 32–43. [[CrossRef](#)]
14. Wang, Z.; Zhao, D.; Guan, Y. Flexible-constrained time-variant hybrid reliability-based design optimization. *Struct. Multidiscip. Optim.* **2023**, *66*, 89. [[CrossRef](#)]
15. Dui, H.; Song, J.; Zhang, Y.A. Reliability and Service Life Analysis of Airbag Systems. *Mathematics* **2023**, *11*, 434. [[CrossRef](#)]
16. Zhang, D.; Shen, S.; Jiang, C.; Han, X.; Li, Q. An advanced mixed-degree cubature formula for reliability analysis. *Comput. Methods Appl. Mech. Eng.* **2022**, *400*, 115521. [[CrossRef](#)]

17. Meng, Z.; Li, H.; Zeng, R.; Mirjalili, S.; Yıldız, A.R. An efficient two-stage water cycle algorithm for complex reliability-based design optimization problems. *Neural Comput. Appl.* **2022**, *34*, 20993–21013. [[CrossRef](#)]
18. Liao, K.W.; Lu, B.C.; Yu, S.P. A Concurrent Approach for a Reliability-Based Optimization Design Problem. *J. Adv. Mech. Des. Syst. Manuf.* **2012**, *6*, 1015–1030. [[CrossRef](#)]
19. Wang, Z.; Zhang, Y.; Song, Y. A modified conjugate gradient approach for reliability-based design optimization. *IEEE Access* **2020**, *8*, 16742–16749. [[CrossRef](#)]
20. Safaeian Hamzehkolaei, N.; Miri, M.; Rashki, M. An enhanced simulation-based design method coupled with meta-heuristic search algorithm for accurate reliability-based design optimization. *Eng. Comput.* **2016**, *32*, 477–495. [[CrossRef](#)]
21. Zhong, C.; Wang, M.; Dang, C.; Ke, W.; Guo, S. First-order reliability method based on Harris Hawks Optimization for high-dimensional reliability analysis. *Struct. Multidiscip. Optim.* **2020**, *62*, 1951–1968. [[CrossRef](#)]
22. Jafari-Asl, J.; Seghier, M.E.A.B.; Ohadi, S.; Correia, J.; Barroso, J. Reliability analysis based improved directional simulation using Harris Hawks optimization algorithm for engineering systems. *Eng. Fail. Anal.* **2022**, *135*, 106148. [[CrossRef](#)]
23. Du, X.P.; Sudjianto, A.; Huang, B.Q. Reliability-based design with the mixture of random and interval variables. *J. Mech. Des.* **2005**, *127*, 1068–1076. [[CrossRef](#)]
24. Zhang, H.; Wang, H.; Wang, Y.; Hong, D. Incremental shifting vector and mixed uncertainty analysis method for reliability-based design optimization. *Struct. Multidiscip. Optim.* **2019**, *59*, 2093–2109. [[CrossRef](#)]
25. Wang, L.; Ma, Y.; Yang, Y.; Wang, X. Structural design optimization based on hybrid time-variant reliability measure under non-probabilistic convex uncertainties. *Appl. Math. Model.* **2019**, *69*, 330–354. [[CrossRef](#)]
26. Van Huynh, T.; Tangaramvong, S.; Do, B.; Gao, W.; Limkatanyu, S. Sequential most probable point update combining Gaussian process and comprehensive learning PSO for structural reliability-based design optimization. *Reliab. Eng. Syst. Saf.* **2023**, *235*, 109164. [[CrossRef](#)]
27. Keshtegar, B.; Chakraborty, S. A hybrid self-adaptive conjugate first order reliability method for robust structural reliability analysis. *Appl. Math. Model.* **2018**, *53*, 319–332. [[CrossRef](#)]
28. Bartocchini, U.; Carpi, A.; Poggioni, V.; Santucci, V. Memes evolution in a memetic variant of particle swarm optimization. *Mathematics* **2019**, *7*, 423. [[CrossRef](#)]
29. Li, J.; Chen, J. Solving time-variant reliability-based design optimization by PSO-t-IRS: A methodology incorporating a particle swarm optimization algorithm and an enhanced instantaneous response surface. *Reliab. Eng. Syst. Saf.* **2019**, *191*, 106580. [[CrossRef](#)]
30. Zhang, Y.; Liu, X.; Li, C. Determining the reasonable state of cable-stayed bridges with twin towers based on multi-objective swarm optimization algorithm. *J. Chang. Univ. Sci. Technol. (Nat. Sci.)* **2019**, *16*, 22–27.
31. Zhu, S.P.; Keshtegar, B.; Seghier, M.E.A.B.; Zio, E.; Taylan, O. Hybrid and enhanced PSO: Novel first order reliability method-based hybrid intelligent approaches. *Comput. Methods Appl. Mech. Eng.* **2022**, *393*, 114730. [[CrossRef](#)]
32. Yu, S.; Wang, Z. A general decoupling approach for time-and space-variant system reliability-based design optimization. *Comput. Methods Appl. Mech. Eng.* **2019**, *357*, 112608. [[CrossRef](#)]
33. Wang, C.; Matthies, H.G. A comparative study of two interval-random models for hybrid uncertainty propagation analysis. *Mech. Syst. Signal Process.* **2020**, *136*, 106531. [[CrossRef](#)]
34. Chopard, B.; Tomassini, M.; Chopard, B.; Tomassini, M. Simulated annealing. In *An Introduction to Metaheuristics for Optimization*; Springer: Berlin/Heidelberg, Germany, 2018; pp. 59–79.
35. Alnowibet, K.A.; Mahdi, S.; El-Alem, M.; Abdelawwad, M.; Mohamed, A.W. Guided hybrid modified simulated annealing algorithm for solving constrained global optimization problems. *Mathematics* **2022**, *10*, 1312. [[CrossRef](#)]
36. Liu, X.; Liu, X.; Zhou, Z.; Hu, L. An efficient multi-objective optimization method based on the adaptive approximation model of the radial basis function. *Struct. Multidiscip. Optim.* **2021**, *63*, 1385–1403. [[CrossRef](#)]
37. Delahaye, D.; Chaimatanan, S.; Mongeau, M. Simulated annealing: From basics to applications. In *Handbook of Metaheuristics*; Springer: Berlin/Heidelberg, Germany, 2019; pp. 1–35.
38. Franzin, A.; Stützle, T. Revisiting simulated annealing: A component-based analysis. *Comput. Oper. Res.* **2019**, *104*, 191–206. [[CrossRef](#)]
39. Liu, X.; Gong, M.; Zhou, Z.; Xie, J.; Wu, W. An improved first order approximate reliability analysis method for uncertain structures based on evidence theory. *Mech. Based Des. Struct. Mach.* **2023**, *51*, 4137–4154. [[CrossRef](#)]
40. Wang, Q.; Huang, Z.; Dong, J. Reliability-based design optimization for vehicle body crashworthiness based on copula functions. *Eng. Optim.* **2020**, *52*, 1362–1381. [[CrossRef](#)]
41. Ai, Q.; Yuan, Y.; Jiang, X.; Wang, H.; Han, C.; Huang, X.; Wang, K. Pathological diagnosis of the seepage of a mountain tunnel. *Tunn. Undergr. Space Technol.* **2022**, *128*, 104657. [[CrossRef](#)]
42. Li, W.; Li, C.; Gao, L.; Xiao, M. Risk-based design optimization under hybrid uncertainties. *Eng. Comput.* **2020**, *38*, 2037–2049. [[CrossRef](#)]
43. Liu, X.; Li, T.; Zhou, Z.; Hu, L. An efficient multi-objective reliability-based design optimization method for structure based on probability and interval hybrid model. *Comput. Methods Appl. Mech. Eng.* **2022**, *392*, 114682. [[CrossRef](#)]
44. Luo, C.; Keshtegar, B.; Zhu, S.P.; Taylan, O.; Niu, X.P. Hybrid enhanced Monte Carlo simulation coupled with advanced machine learning approach for accurate and efficient structural reliability analysis. *Comput. Methods Appl. Mech. Eng.* **2022**, *388*, 114218. [[CrossRef](#)]

45. Liu, X.; Lai, H.; Wang, X.; Song, X.; Liu, K.; Wu, S.; Li, Q.; Wang, F.; Zhou, Z. Aerospace Structural Reliability Analysis Method Based on Regular Vine Copula Model with the Asymmetric Tail Correlation. *Aerosp. Sci. Technol.* **2023**, *142*, 108670. [[CrossRef](#)]
46. Thakkar, A.; Lohiya, R. A survey on intrusion detection system: Feature selection, model, performance measures, application perspective, challenges, and future research directions. *Artif. Intell. Rev.* **2022**, *55*, 453–563. [[CrossRef](#)]
47. Wang, Y.H.; Zhang, C.; Su, Y.Q.; Shang, L.Y.; Zhang, T. Structure optimization of the frame based on response surface method. *Int. J. Struct. Integr.* **2019**, *11*, 411–425. [[CrossRef](#)]
48. Yang, S.; Meng, D.; Wang, H.; Chen, Z.; Xu, B. A comparative study for adaptive surrogate-model-based reliability evaluation method of automobile components. *Int. J. Struct. Integr.* **2023**, *14*, 498–519. [[CrossRef](#)]
49. Meng, D.; Yang, S.; de Jesus, A.M.; Zhu, S.P. A novel Kriging-model-assisted reliability-based multidisciplinary design optimization strategy and its application in the offshore wind turbine tower. *Renew. Energy* **2023**, *203*, 407–420. [[CrossRef](#)]
50. Chen, J.; Zhang, X.; Jing, Z. A cooperative PSO-DP approach for the maintenance planning and RBDO of deteriorating structures. *Struct. Multidiscip. Optim.* **2018**, *58*, 95–113. [[CrossRef](#)]
51. Lai, X.; Huang, J.; Zhang, Y.; Wang, C.; Zhang, X. A general methodology for reliability-based robust design optimization of computation-intensive engineering problems. *J. Comput. Des. Eng.* **2022**, *9*, 2151–2169. [[CrossRef](#)]
52. Qiang, C.; Deng, Y. A new correlation coefficient of mass function in evidence theory and its application in fault diagnosis. *Appl. Intell.* **2022**, *52*, 7832–7842. [[CrossRef](#)]
53. Ai, Q.; Yuan, Y.; Shen, S.L.; Wang, H.; Huang, X. Investigation on inspection scheduling for the maintenance of tunnel with different degradation modes. *Tunn. Undergr. Space Technol.* **2020**, *106*, 103589. [[CrossRef](#)]
54. Gao, J.W.; Dai, X.; Zhu, S.P.; Zhao, J.W.; Correia, J.A.; Wang, Q. Failure causes and hardening techniques of railway axles—A review from the perspective of structural integrity. *Eng. Fail. Anal.* **2022**, *141*, 106656. [[CrossRef](#)]
55. Yang, S.; Meng, D.; Wang, H.; Yang, C. A novel learning function for adaptive surrogate-model-based reliability evaluation. *Philos. Trans. R. Soc. A* **2023**, *382*, 20220395. [[CrossRef](#)] [[PubMed](#)]
56. Xiong, L.; Su, X.; Qian, H. Conflicting evidence combination from the perspective of networks. *Inf. Sci.* **2021**, *580*, 408–418. [[CrossRef](#)]
57. Yu, S.; Li, Y. Active learning kriging model with adaptive uniform design for time-dependent reliability analysis. *IEEE Access* **2021**, *9*, 91625–91634. [[CrossRef](#)]
58. Gao, X.; Su, X.; Qian, H.; Pan, X. Dependence assessment in human reliability analysis under uncertain and dynamic situations. *Nucl. Eng. Technol.* **2022**, *54*, 948–958. [[CrossRef](#)]
59. Meng, Z.; Keshtegar, B. Adaptive conjugate single-loop method for efficient reliability-based design and topology optimization. *Comput. Methods Appl. Mech. Eng.* **2019**, *344*, 95–119. [[CrossRef](#)]
60. Li, W.; Xiao, M.; Garg, A.; Gao, L. A New Approach to Solve Uncertain Multidisciplinary Design Optimization based on Conditional Value at Risk. *IEEE Trans. Autom. Sci. Eng.* **2021**, *18*, 356–368. [[CrossRef](#)]
61. Meng, D.; Yang, S.; Lin, T.; Wang, J.; Yang, H.; Lv, Z. RBMDO using gaussian mixture model-based second-order mean-value saddlepoint approximation. *Comput. Model. Eng. Sci.* **2022**, *132*, 553–568. [[CrossRef](#)]
62. Li, X.Q.; Song, L.K.; Bai, G.C. Recent advances in reliability analysis of aeroengine rotor system: A review. *Int. J. Struct. Integr.* **2021**, *13*, 1–29. [[CrossRef](#)]
63. Yang, S.; Meng, D.; Guo, Y.; Nie, P.; Jesus, A.M.D. A reliability-based design and optimization strategy using a novel MPP searching method for maritime engineering structures. *Int. J. Struct. Integr.* **2023**, *14*, 809–826. [[CrossRef](#)]
64. Lu, L.; Wu, Y.; Zhang, Q.; Qiao, P. A Transformation-Based Improved Kriging Method for the Black Box Problem in Reliability-Based Design Optimization. *Mathematics* **2023**, *11*, 218. [[CrossRef](#)]
65. Song, L.K.; Bai, G.C.; Li, X.Q.; Wen, J. A unified fatigue reliability-based design optimization framework for aircraft turbine disk. *Int. J. Fatigue* **2021**, *152*, 106422. [[CrossRef](#)]
66. Song, X.; Xiao, F. Combining time-series evidence: A complex network model based on a visibility graph and belief entropy. *Appl. Intell.* **2022**, *52*, 10706–10715. [[CrossRef](#)]
67. Song, K.; Zhang, Y.; Zhuang, X.; Yu, X.; Song, B. Reliability-based design optimization using adaptive surrogate model and importance sampling-based modified SORA method. *Eng. Comput.* **2021**, *37*, 1295–1314. [[CrossRef](#)]
68. Wang, Z.; Xiao, F.; Cao, Z. Uncertainty measurements for Pythagorean fuzzy set and their applications in multiple-criteria decision making. *Soft Comput.* **2022**, *26*, 9937–9952. [[CrossRef](#)]
69. Dunn, W.L.; Shultis, J.K. *Exploring Monte Carlo Methods*, 3rd ed.; Elsevier: Burlington, MA, USA, 2012; pp. 154–196.
70. Liang, J.; Mourelatos, Z.P.; Tu, J. A single-Loop method for reliability-based design optimization. *Proc. ASME Des. Eng. Tech. Conf.* **2004**, *1*, 419–430.
71. Azarm, S.; Li, W.C. Multi-level design optimization using global monotonicity analysis. *J. Mech. Transm. Autom. Des.* **1989**, *111*, 259–263. [[CrossRef](#)]
72. Gunawan, S.; Azarm, S.; Wu, J.; Boyars, A. Quality-assisted multi-objective multidisciplinary genetic algorithms. *Aiaa J.* **2003**, *41*, 1752–1762. [[CrossRef](#)]

Disclaimer/Publisher’s Note: The statements, opinions and data contained in all publications are solely those of the individual author(s) and contributor(s) and not of MDPI and/or the editor(s). MDPI and/or the editor(s) disclaim responsibility for any injury to people or property resulting from any ideas, methods, instructions or products referred to in the content.